

# Tunable soy protein isolate hydrogel for nanoparticles brain release

Received: 2 February 2026

Accepted: 12 May 2026

Cite this article as: Ciprandi, M., Fontanini, V., Sommi, P. *et al.* Tunable soy protein isolate hydrogel for nanoparticles brain release. *J Mater Sci: Mater Med* (2026). <https://doi.org/10.1007/s10856-026-07072-9>

Matilde Ciprandi, Veronica Fontanini, Patrizia Sommi, Umberto Anselmi-Tamburini, Silvia Sesana & Francesca Re

We are providing an unedited version of this manuscript to give early access to its findings. Before final publication, the manuscript will undergo further editing. Please note there may be errors present which affect the content, and all legal disclaimers apply.

If this paper is publishing under a Transparent Peer Review model then Peer Review reports will publish with the final article.

**Tunable soy protein isolate hydrogel for nanoparticles brain release****Authors**

Matilde Ciprandi<sup>1\*</sup>, Veronica Fontanini<sup>1\*</sup>, Patrizia Sommi<sup>2</sup>, Umberto Anselmi-Tamburini<sup>3</sup>, Silvia Sesana<sup>1</sup>, Francesca Re<sup>1,4</sup>

<sup>1</sup> School of Medicine and Surgery, University of Milano-Bicocca, Monza, Italy

<sup>2</sup> Department of Molecular Medicine, University of Pavia, Pavia, Italy

<sup>3</sup> Department of Chemistry, University of Pavia, Pavia, Italy

<sup>4</sup> Fondazione IRCCS San Gerardo dei Tintori, 20900, Monza, Italy

\* Equally contribution

Correspondence to: francesca.re1@unimib.it

## Abstract

Implantable biomaterials for local drug release have been investigated to avoid the need to cross the blood-brain barrier, which is one of the major limitations of current brain tumors therapies. However, their translation is still limited by inadequate tissue compatibility and suboptimal drug/nanoparticles release. In this study, soy protein isolate (SPI) hydrogels were engineered using microbial transglutaminase (MTGase) as a safe, naturally derived crosslinker, and optimized for brain-relevant constraints. Hydrogels were prepared at 10% and 12% (w/v) SPI and crosslinked with 20 or 40 mg MTGase/g SPI. Crosslinking was confirmed by SDS-PAGE, while scanning electron microscopy revealed a highly porous, microstructure with well-defined cavities. Hydrogels showed high water content (87-89%) and controlled swelling behaviour over 72 h that is inversely correlated to MTGase concentration. Rheological analysis demonstrated solid-like behaviour ( $G' > G''$ ), shear-thinning viscosity suitable for syringe-based injection, and mechanical stability under dynamic stress. Among the tested samples, the 10% (w/v) SPI hydrogel crosslinked with 20 mg MTGase/g SPI exhibited a storage modulus (~260 Pa) closely matching native brain tissue, making it the most suitable candidate for intracranial application. This formulation enabled controlled release of 100–200 nm liposomes and sustained delivery of doxorubicin-loaded liposomes, resulting in a significant reduction in glioblastoma cell viability *in vitro*. Importantly, the hydrogel showed no cytotoxicity and did not allow cancer cell adhesion and infiltration, confirming its bioinert nature. Overall, MTGase-crosslinked SPI hydrogels emerge as versatile, scalable, and brain-compatible biomaterials for injectable implants and sustained local nanoparticle release.

## Keywords

Hydrogel, liposomes, brain, biomaterial, soy protein.

## Introduction

Glioblastoma multiforme (GBM) remains one of the most aggressive and treatment-resistant brain tumors, with high recurrence rates [1]. One of the major limitations of current therapies is the inefficient delivery of drugs to residual infiltrative tumor cells, largely due to the blood-brain barrier (BBB) [2]. Despite the clinical success of nanomedicine, no nanoparticle-based therapy has yet been approved for brain cancers [3–5]. This highlights the urgent need for locally administered therapeutic strategies specifically engineered for the unique biological and physical properties of the brain microenvironment. Implantable biomaterials have been investigated to avoid reliance on the BBB crossing, but their translation is still limited by inadequate tissue compatibility and suboptimal drug/nanoparticles release [2]. In our previous work, we reported the design and characterization of soy protein isolate (SPI) hydrogels for the sustained release of nanoparticles [2]. Building on these findings, this manuscript focuses on improving the hydrogel design by optimizing formulation parameters to align with brain-relevant mechanical, rheological, and bioinert requirements. We employed the naturally occurring enzyme, microbial transglutaminase MTGase, to confer tunable characteristics to the hydrogels. This work provides a significant step forward in the rational design of brain-adapted, sustainable biomaterials for local GBM therapy.

## Materials and Methods

Hydrogels were prepared by dissolving 10-12% w/v SPI (MP Biomedicals, LLC) in Milli-Q water containing 20 or 40 mg of MTGase (BDF Ingredients)/g SPI. The mixture was then homogenized using an Ultra-Turrax T25 at 12,000 rpm for 5 minutes, divided into 24-well plates (0.5 g/well) and incubated for 1h at 37°C, 5%CO<sub>2</sub> to allow gelation. To verify the activity of MTGase, samples were incubated for 1 or 24h at 37°C, 5%CO<sub>2</sub>, then heated at 100°C, and an aliquot (25 µg total proteins) was analyzed by SDS-PAGE (4-12% Bis-Tris gel, MOPS buffer). Protein bands were stained with EZ-Blue and visualized with Amersham Imager 600. The morphology of hydrogels was analysed by scanning electron microscopy

(SEM) imaging. To assess the water absorption capacity of SPI, hydrogels were weighed before and after lyophilization. The percentage of absorbed water was calculated as described [2].

The swelling capacity of the hydrogels was assessed by adding 2 mL of Milli-Q water and incubating the samples at 37°C, 5%CO<sub>2</sub> for up to 72h. The swelling percentage was calculated as described [2].

The hydrolytic degradation was assessed by measuring the protein released from hydrogels/total hydrogel protein content with BCA assay (Thermo Fisher Scientific). The mechanical properties of hydrogels (amplitude sweep, viscosity, and frequency sweep) were evaluated on a rheometer (Modular Compact Rheometer RCM 72) with a flat disc, applying a shear rate between 0.1 and 1000 s<sup>-1</sup>, at 37°C. Storage Modulus (G') and Loss Modulus (G'') were compared with the values reported in the literature for brain tissue.

To validate hydrogels as biomaterial for controlled local release of nanoparticles, sphingomyelin/cholesterol (1:1 mol/mol) liposomes (conventional or loaded with doxorubicin, Lipo-doxo, as drug model) of different diameters were prepared by lipid film hydration in D-PBS, followed by extrusion, following the procedure described [6]. After physico-chemical characterization [7], liposomes (200µM total lipids) were added to hydrogels before gelation, and their release was measured at 37°C, 5%CO<sub>2</sub> for up to 72h using Nanoparticle Tracking Analysis NTA (Nanosight, Malvern Panalytical).

To check if Lipo-doxo release from the hydrogels maintains their therapeutic activity, U87-MG and Gli36ΔEGFR-2 GBM-like cell lines were used as *in vitro* models of glioblastoma. Cells were cultured accordingly to the described procedure [2,8] and seeded (30,000 cells/well) in the lower compartment of a transwell system (Greiner BioOne). Hydrogels loaded with Lipo-doxo (400µM total lipids) were gelled directly on the filter, and the apical compartment was filled with artificial cerebrospinal fluid [2]. Cell viability was assessed 72h after incubation at 37°C, 5%CO<sub>2</sub> by MTT assay [9].

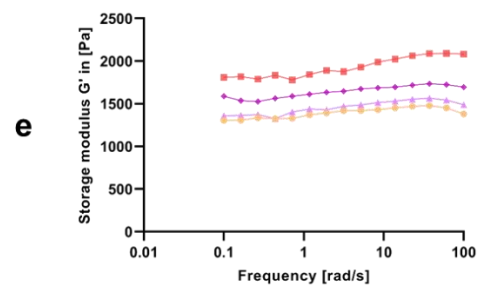
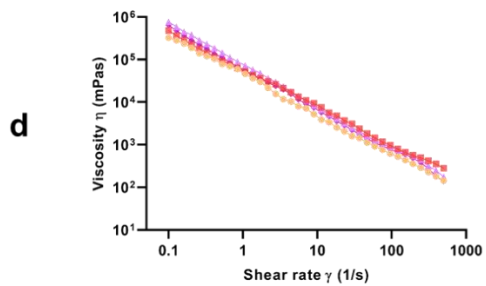
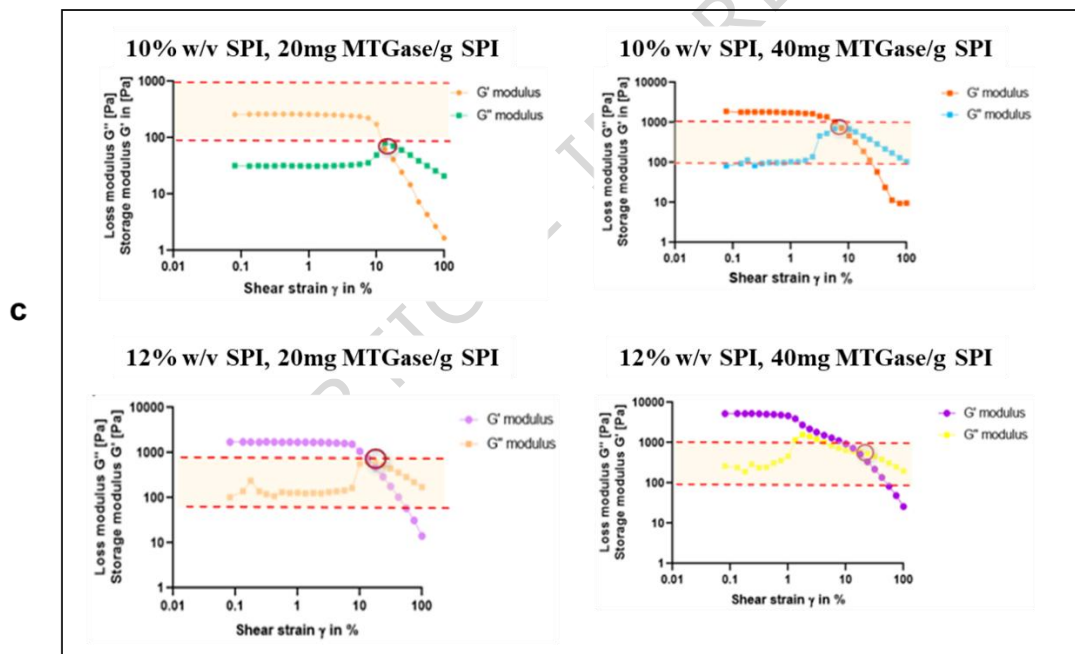
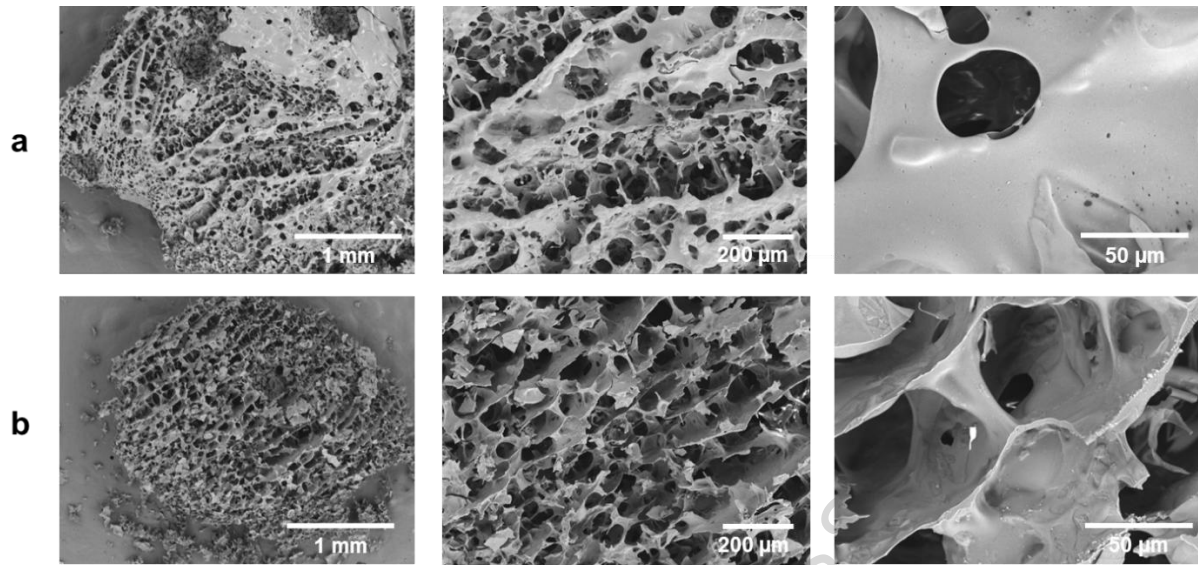
To evaluate the hydrogel's resistance to cell adhesion and infiltration, GBM cells (20,000 cells/well) were seeded onto pre-gelled, fluorescent-labelled hydrogel (0.1mM Rhodamine B, Sigma-Aldrich) in 96-well plates. After 72h of incubation at 37°C, 5% CO<sub>2</sub>, cell membranes were stained with wheat germ agglutinin (1:300, Invitrogen) for 20 minutes, and nuclei with Hoechst (1:1000, Invitrogen) for 5 minutes. Imaging was performed using the Operetta CLS High Content Analysis System. Statistical analyses were performed using GraphPad Prism 8, by One-way ANOVA ( $p < 0.05$ ).

## Results

Hydrogels were prepared at two SPI concentrations (10% and 12% w/v), cross-linked with 20 or 40 mg of MTGase/g SPI, and their suitability for brain-relevant constraints [10] was evaluated. The cross-linking was confirmed by the significant decrease in the intensity of the major SPI subunit bands, using SDS-PAGE

(Fig. SI 1), accordingly to previous reports [11]. The SEM images reveal a highly porous, interconnected microstructure spanning multiple length scales. At lower magnification, the hydrogel exhibits a heterogeneous, sponge-like architecture, while higher-magnification views show smooth pore walls and well-defined cavities (Fig. 1a-b).

ARTICLE IN PRESS



—●— 10% w/v SPI, 20mg MTGase/g SPI  
 —■— 10% w/v SPI, 40mg MTGase/g SPI

—▲— 12% w/v SPI, 20mg MTGase/g SPI  
 —◆— 12% w/v SPI, 40mg MTGase/g SPI

**Figure 1 SEM analysis of hydrogels.** The hydrogels were prepared in a Petri dish and then freeze-dried, before undergoing scanning electron microscopy (SEM) analysis using a TESCAN Mira 3 XMU microscope (TESCAN ORSAY HOLDING s.a., Czech Republic) equipped with a field emission source, operated at 5 kV using its In-Beam SE (secondary electrons) model. Images were acquired at multiple magnifications. **a)** Representative images of the 10% w/v SPI, 20mg MTGase/g SPI hydrogels are shown. **b)** Representative images of the 10% w/v SPI, 40mg MTGase/g SPI hydrogels are shown. Scale bars are embedded in the images. **c-e)** Rheological characterization of SPI hydrogels. Hydrogel physical and mechanical properties were characterized through rheological tests on a rotational rheometer. **c)** The amplitude sweep test evaluates the hydrogel's mechanical properties by applying progressively increasing deformation. The resulting elastic (Storage) modulus ( $G'$ ) and viscous (Loss) modulus ( $G''$ ) curves are obtained under controlled shear strain. Brain tissue  $G'$  interval (0.1-1 kPa) is highlighted. **d)** The steady-state flow test revealed pronounced shear-thinning behaviour. **e)** A frequency sweep test was performed to assess how the hydrogel responds to constant deformation at increasing frequencies. Data are presented as the mean  $\pm$  SD of at least three replicates.

10% w/v SPI hydrogels showed a higher water content ( $89 \pm 0.5\%$ ) compared to 12% w/v hydrogels ( $87 \pm 0.2\%$ ), despite variations in MTGase concentration (Fig. SI 2a). To predict the behaviour of hydrogels in aqueous fluids, the swelling capacity was evaluated over 72 h. 10% w/v SPI hydrogels exhibited a lower swelling % compared to 12% w/v (Fig. SI 2b), and the swelling was inversely correlated with MTGase concentrations. Considering that the % swelling is affected by the hydrolytic degradation of the hydrogel, BCA assay was used to quantify SPI released. All hydrogels exhibited an initial burst release of 35 % within 24 h, which is likely due to rapid water absorption that corresponds to the higher % of swelling (Fig. SI 2c). To determine the mechanical and rheological properties of hydrogels,  $G'$  and  $G''$  moduli were measured through amplitude sweep, frequency sweep, and viscosity tests. Results showed that  $G' > G''$  for all samples until the crossover point. The 10% w/v SPI, 20mg MTGase/g SPI hydrogel displayed a  $G' \approx 260$  Pa, whereas all the other samples exceeded 1000 Pa. Additionally,  $G'$  increased proportionally with enzyme concentration (Fig. 1c). Viscosity tests showed a decrease of 4 orders of magnitude as the shear rate increased ( $0.1$  to  $1000 \text{ s}^{-1}$ ) for all hydrogels (Fig. 1d), as reported for other types of hydrogels [9,10]. Furthermore, frequency sweep tests demonstrated that  $G'$  remained constant over the tested range (Fig. 1e). Based on these results, 10% w/v SPI, 20mg MTGase/g SPI hydrogel was chosen as the best candidate and further characterized for nanoparticles release. In order to determine the optimal size of nanoparticles to allow their release from hydrogel, liposomes of different diameters were prepared, characterized (Fig. SI 3a), loaded in hydrogels, and their release was measured over time by NTA. Results showed that 100 and 200 nm sized liposome were released in a controlled time manner, with a kinetic release of  $1.15 \times 10^{10}$  liposome/h (Fig. 2a, Fig. SI 3b).

To assess the applicability of hydrogel as reservoir for controlled release of therapeutic nanoparticles, Lipodoxo (130 nm diameter,  $\text{PDI} < 0.2$ , doxo encapsulation efficiency  $84 \pm 11\%$ ) were loaded into hydrogel, and the efficacy was validated using an *in vitro* transwell system (Fig. 2b). After 72h, a significant reduction in

cancer cell viability was measured (Fig. 2c-d), confirming that released liposomes maintain their pharmacological activity. No cytotoxicity was detected after cell incubation with empty hydrogels. Finally, to evaluate whether the hydrogel does not allow cell adhesion and infiltration, GBM-like cells stained with WGA and Hoechst were seeded on Rhodamine B-labeled hydrogels and examined using confocal microscopy. Images showed that the hydrogel do not allow cancer cells adhesion or infiltration (Fig. 2e-f).

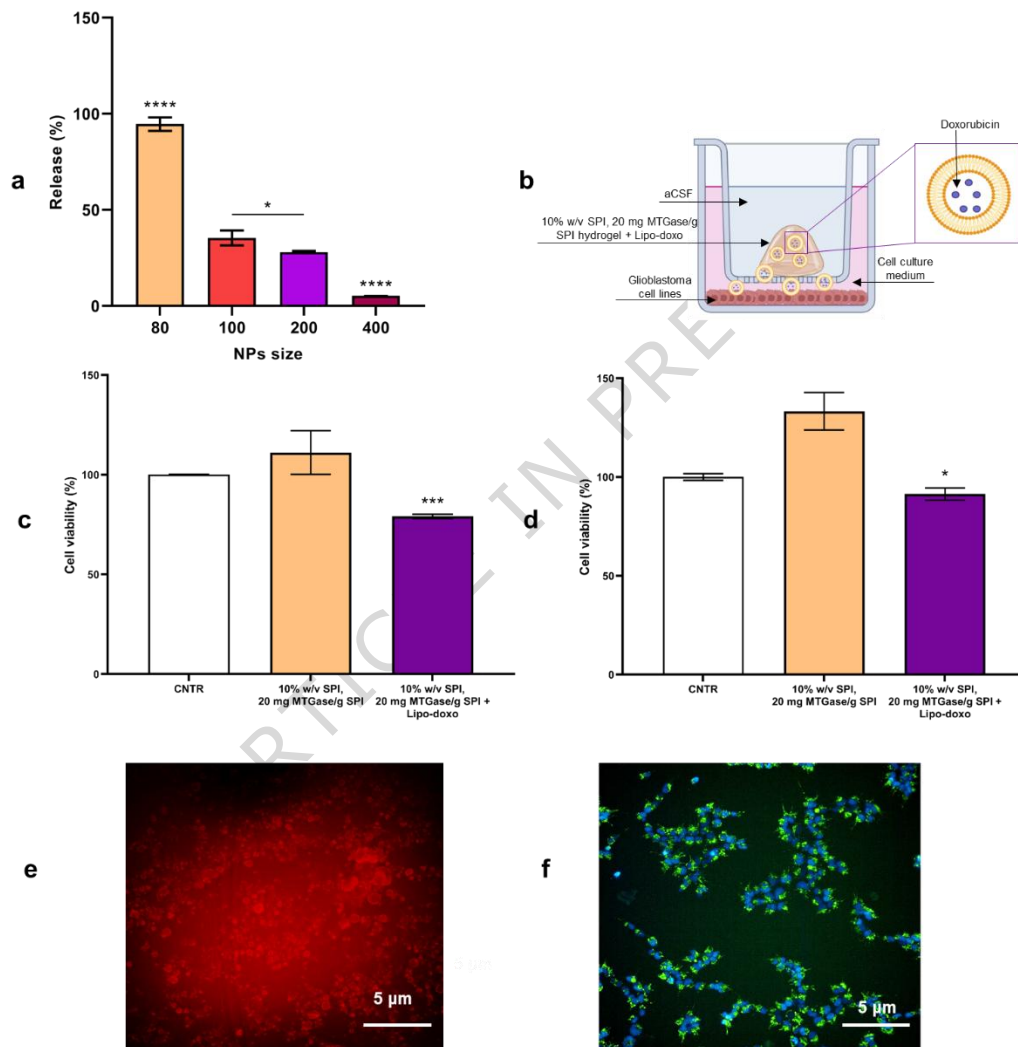


**Figure 2 Validation of hydrogels as reservoir for controlled release of therapeutic nanoparticles. a)** Release (%) of liposomes of different diameters (80, 100, 200, 400 nm) from 10% w/v SPI, 20 mg MTGase/g SPI hydrogel in 24 h, at 37°C. After gelation, hydrogels loaded with liposomes were incubated in Milli-Q water for 24 h, then the Milli-Q water was collected, centrifuged for 30 minutes to remove SPI and the number of released liposomes were measured by NTA. **b)** Schematic representation of the *in vitro* transwell system (24-well format, 0.4  $\mu$ m polyester membrane). Glioblastoma cells (U87-MG or Gli36 $\Delta$ EGFR-2) were cultured in the lower compartment (30,000 cells/well). In the upper compartment, the hydrogel loaded or not with Lipo-doxo was placed on the membrane filter. **c)** Cell viability of U87-MG cells after 72 h of treatment with empty hydrogel or Lipo-doxo-loaded hydrogel, assessed by MTT assay. **d)** Cell viability of Gli36 $\Delta$ EGFR-2 cells after 72 h of treatment with empty hydrogel or Lipo-doxo-loaded hydrogel, assessed by MTT assay. Data are expressed as a mean  $\pm$  standard deviation. \*,  $p < 0.05$ ; \*\*\*,  $p < 0.001$

(One-way ANOVA). GBM cells seeded in transwell without hydrogels in the upper compartment were used as control. **e-f)** Assessment of tumor cell adhesion and infiltration into the hydrogel. Gli36 $\Delta$ EGFR-2 cells (20,000 cells/well) were seeded onto pre-gelled, fluorescent-labelled 10% w/v SPI, 20 mg MTGase/g SPI hydrogel (0.1mM Rhodamine B, red staining) in 96-well plates. After 72h of incubation at 37°C, 5%CO<sub>2</sub>, cell membranes were stained with wheat germ agglutinin (1:300, green staining) for 20 minutes, and nuclei with Hoechst (1:1000, blue staining) for 5 minutes. Imaging was performed using the Operetta CLS High Content Analysis System and analyzed using Fiji ImageJ. Gli36 $\Delta$ EGFR-2 cells seeded in 96-well plates with hydrogels (e); no cells were detectable. Gli36 $\Delta$ EGFR-2 cells seeded in 96-well plates without hydrogels were used as control (f). Scale bars are embedded in the figure.

## Discussion

Taken together, the results highlight the effective and tunable cross-linking of SPI hydrogels mediated by MTGase, leading to the formation of dense yet adaptable polymer networks. In particular, the higher water content observed in 10% w/v SPI hydrogels contributes to enhanced flexibility and softness [12], while their reduced swelling behaviour represents a critical advantage for intracranial applications, where excessive volumetric expansion may result in increased intracranial pressure. From a structural standpoint, a lower cross-linking density promotes network expansion and increases the free volume available for water uptake, a feature that is expected to favour nanoparticle accommodation and diffusion within the hydrogel matrix. Rheological characterization confirmed the solid-like nature of all formulations, with the storage modulus ( $G'$ ) consistently exceeding the loss modulus ( $G''$ ) up to the crossover point. Importantly, the elastic response of the hydrogels could be finely tuned by modulating the MTGase concentration, as evidenced by the proportional increase in  $G'$  with enzyme content. Among the tested formulations, the 10% w/v SPI hydrogel cross-linked with 20mg MTGase/g SPI exhibited mechanical properties closely matching those of native brain tissue ( $G' \approx 0.1-1$  kPa [2]), identifying this formulation as the most suitable candidate for intracranial implantation and localized nanoparticle release. All hydrogels displayed a pronounced shear-thinning behaviour, with viscosity decreasing by approximately four orders of magnitude as the shear rate increased from 0.1 to 1000 s<sup>-1</sup>, in agreement with previous reports on injectable hydrogel systems [9,10]. This property is essential for minimally invasive, syringe-based administration, enabling in situ gel placement while preserving the structural integrity of the encapsulated nanoparticles. Moreover, frequency sweep tests showed that  $G'$  remained nearly constant over the tested range, indicating high mechanical stability under varying dynamic stresses. Finally, confocal imaging analyses revealed that the SPI hydrogels did not support cancer cell adhesion or infiltration, confirming their bioinert character. This feature is particularly relevant for intracranial applications, as it suggests that the hydrogel matrix can act as a

mechanically compliant and biologically inert reservoir for the controlled and localized release of nanoparticles within the brain.

## **Conclusion**

In conclusion, this work demonstrates that MTGase, a safe and naturally derived enzyme, is an effective cross-linker to engineer SPI-based hydrogels with tunable structural, swelling, mechanical, and rheological properties. By modulating SPI and enzyme concentrations, hydrogels can be tailored to match the stringent physicochemical characteristics of brain tissue, including low stiffness, limited swelling, injectability, mechanical stability and biocompatibility. The selected formulation closely matched brain-like viscoelasticity, prevented cell infiltration, and enabled controlled nanoparticle release while preserving drug-embedded activity. Altogether, these results highlight MTGase-crosslinked SPI hydrogels as promising, versatile, and scalable candidates for brain implant and local drug delivery applications. However, alternative crosslinkers, longer-term degradation and release studies, and *in vivo* validation will be further investigated to strengthen the translational potential of this approach.

## **Acknowledgements**

We thank Evelyn Ochoa and Miriam Colombo from the Department of Biotechnology and Biosciences, University of Milano-Bicocca, for the support in rheological measurements and Centro Interdipartimentale di Studi e Ricerca per la Conservazione del Patrimonio Culturale (CISRIC), University of Pavia, for providing access to SEM.

## **Funding**

This work was supported by Fondo di Ateneo 2020-2021, University Milano Bicocca (ATE): “Design of hydrogel for controlled release of drug-loaded nanoparticles as therapeutic approach against Glioblastoma recurrence”.

## **Competing interests**

The authors declare that they have no known competing financial interests.

## **Author contributions**

Preparation, characterization of hydrogels, *in vitro* experiments on cells, data analysis and curation, preparation of figures, writing of manuscript draft, MC and VF. SEM imaging, PS and UAT. Data curation,

SS. Data curation, writing-review and editing of manuscript, FR, PS, and UAT. Conceptualization, data curation, writing—review and editing, funding acquisition, FR.

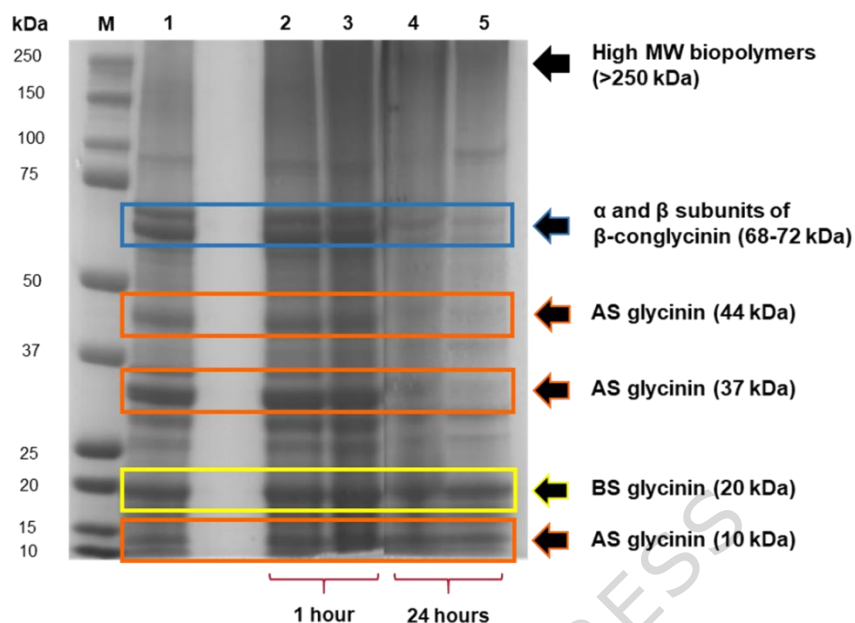
## References

- [1] Singh S, Dey D, Barik D, Mohapatra I, Kim S, Sharma M, et al. Glioblastoma at the crossroads: current understanding and future therapeutic horizons. *Sig Transduct Target Ther* 2025;10:213. <https://doi.org/10.1038/s41392-025-02299-4>.
- [2] Viale F, Ciprandi M, Leoni L, Sierrri G, Renda A, Barbugian F, et al. Biodegradable SPI-based hydrogel for controlled release of nanomedicines: A potential approach against brain tumors recurrence. *Journal of Drug Delivery Science and Technology* 2024;96:105672. <https://doi.org/10.1016/j.jddst.2024.105672>.
- [3] Taiarol L, Formicola B, Magro RD, Sesana S, Re F. An Update of Nanoparticle-Based Approaches for Glioblastoma Multiforme Immunotherapy. *Nanomedicine* 2020;15:1861–71. <https://doi.org/10.2217/nnm-2020-0132>.
- [4] Si J-X, Liu Z-C, Gu F, Jin X, Ma Y-Y. Nanoparticle-based delivery systems for targeted therapy in brain tumors: Progress, challenges and perspectives (Review). *International Journal of Oncology* 2025;67:1–15. <https://doi.org/10.3892/ijo.2025.5789>.
- [5] Sierrri G, Patrucco M, Ferrario D, Renda A, Comi S, Ciprandi M, et al. Targeting specific brain districts for advanced nanotherapies: A review from the perspective of precision nanomedicine. *WIREs Nanomedicine and Nanobiotechnology* 2024;16:e1991. <https://doi.org/10.1002/wnan.1991>.
- [6] Pizzocri M, Re F, Stanzani E, Formicola B, Tamborini M, Lauranzano E, et al. Radiation and adjuvant drug-loaded liposomes target glioblastoma stem cells and trigger in-situ immune response. *Neuro Oncol Adv* 2021;3:vdab076. <https://doi.org/10.1093/oaajnl/vdab076>.
- [7] Conti E, Gregori M, Radice I, Da Re F, Grana D, Re F, et al. Multifunctional liposomes interact with Abeta in human biological fluids: Therapeutic implications for Alzheimer's disease. *Neurochemistry International* 2017;108:60–5. <https://doi.org/10.1016/j.neuint.2017.02.012>.
- [8] Sierrri G, Saenz-de-Santa-Maria I, Renda A, Koch M, Sommi P, Anselmi-Tamburini U, et al. Nanoparticle shape is the game-changer for blood–brain barrier crossing and delivery through tunneling nanotubes among glioblastoma cells. *Nanoscale* 2025;17:992–1006. <https://doi.org/10.1039/D4NR03174A>.
- [9] Sierrri G, Saenz-de-Santa-Maria I, Renda A, Koch M, Sommi P, Anselmi-Tamburini U, et al. Nanoparticle shape is the game-changer for blood–brain barrier crossing and delivery through

- tunneling nanotubes among glioblastoma cells. *Nanoscale* 2025;17:992–1006. <https://doi.org/10.1039/D4NR03174A>.
- [10] Bastiancich C, Danhier P, Pr at V, Danhier F. Anticancer drug-loaded hydrogels as drug delivery systems for the local treatment of glioblastoma. *Journal of Controlled Release* 2016;243:29–42. <https://doi.org/10.1016/j.jconrel.2016.09.034>.
- [11] Tang C-H, Wu H, Yu H-P, Li L, Chen Z, Yang X-Q. Coagulation and Gelation of Soy Protein Isolates Induced by Microbial Transglutaminase. *Journal of Food Biochemistry* 2006;30:35–55. <https://doi.org/10.1111/j.1745-4514.2005.00049.x>.
- [12] Chien KB, Chung EJ, Shah RN. Investigation of soy protein hydrogels for biomedical applications: Materials characterization, drug release, and biocompatibility. *J Biomater Appl* 2014;28:1085–96. <https://doi.org/10.1177/0885328213497413>.
- [13] Hu C, Hahn L, Yang M, Altmann A, Stahlhut P, Groll J, et al. Improving printability of a thermoresponsive hydrogel biomaterial ink by nanoclay addition. *J Mater Sci* 2021;56:691–705. <https://doi.org/10.1007/s10853-020-05190-5>.
- [14] Paxton N, Smolan W, B ock T, Melchels F, Groll J, Jungst T. Proposal to assess printability of bioinks for extrusion-based bioprinting and evaluation of rheological properties governing bioprintability. *Biofabrication* 2017;9:044107. <https://doi.org/10.1088/1758-5090/aa8dd8>.

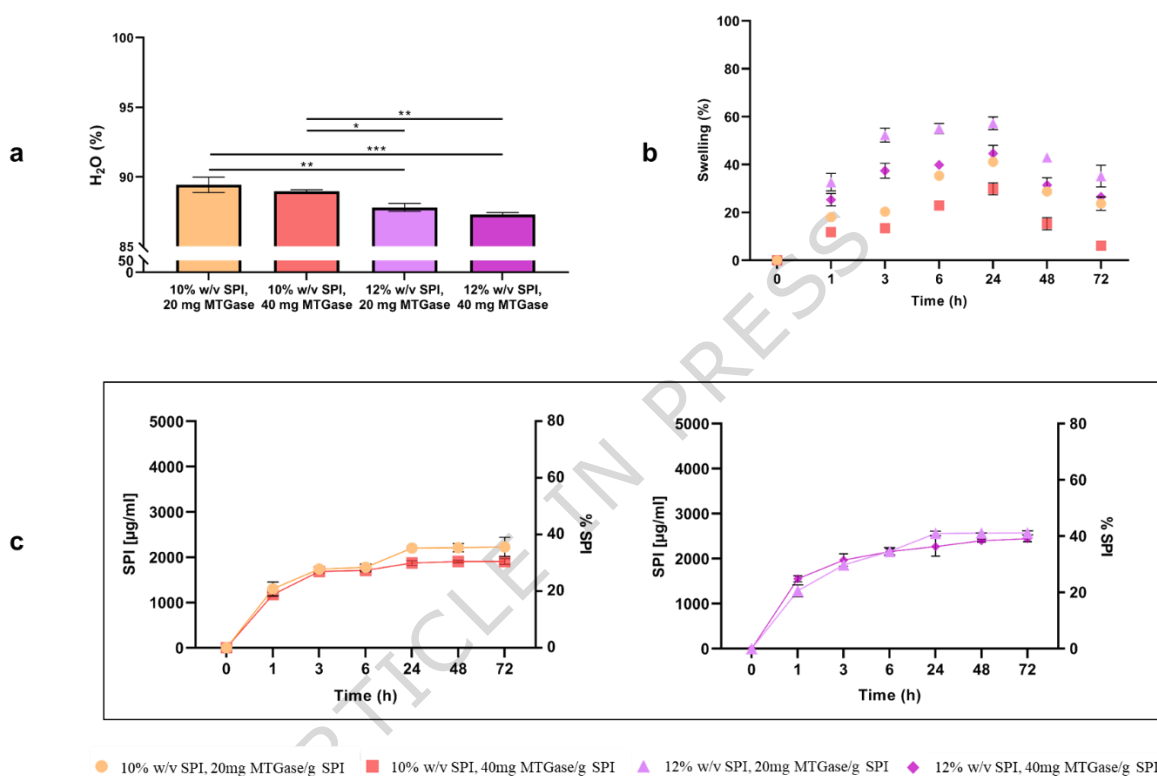
## SUPPLEMENTARY INFORMATION

### Figure SI 1



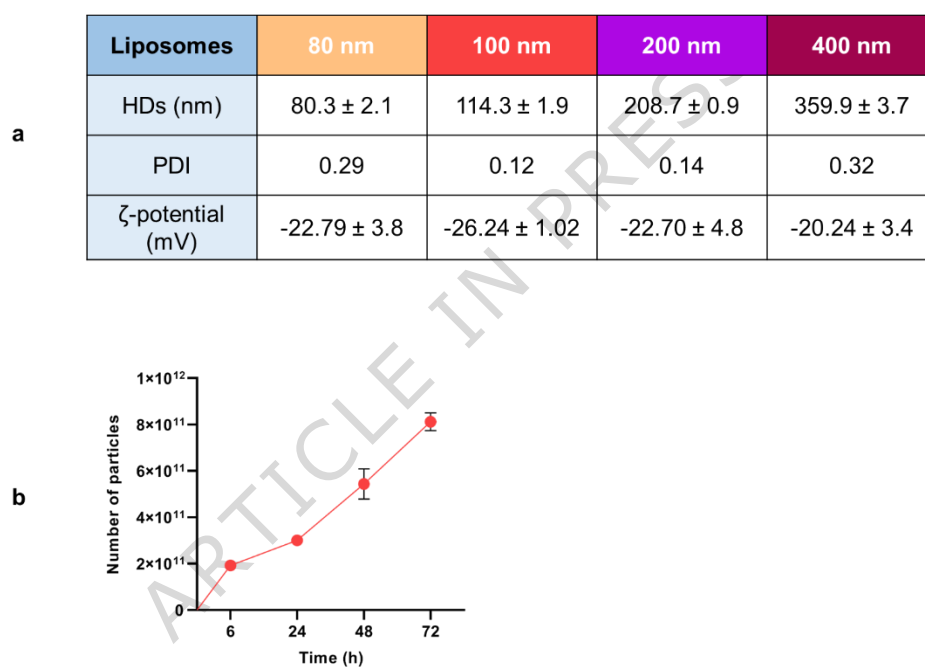
**Figure SI 1** Electrophoretic profile of 12% w/v SPI in Milli-Q water following incubation at 37 °C, 5% CO<sub>2</sub> with 20 or 40 mg MTGase/g SPI for 1 or 24 h. Samples were resolved on a pre-cast 4-12% Bis-Tris gel and stained with EZ-Blue. The progressive disappearance of native SPI subunits and the appearance of high-molecular-weight bands illustrate MTGase-induced polymerization, leading to the formation of new biopolymers suitable for producing hydrogels with controlled pore size. Lanes: M, marker of MW; 1, only SPI; 2, SPI treated with 20 mg of MTGase/g SPI for 1 hour; 3, SPI treated with 40 mg of MTGase/g SPI for 1 hour; 4, SPI treated with 20 mg of MTGase/g SPI for 24 hours; 5, SPI treated with 40 mg of MTGase/g SPI for 24 hours.

Figure SI 2



**Figure SI 2 Physicochemical characterization of hydrogels. a)** % of water absorption from hydrogels prepared with 10% and 12% w/v SPI and crosslinked with 20 or 40 mg MTGase/g SPI. After gelation, the hydrogels were weighed, frozen, and lyophilized to obtain their dry weight. The weight difference between the initial and dry weights enabled the calculation of water uptake. Results showed 89% for the 10% SPI hydrogels and 87% for 12% SPI hydrogels. **b)** Swelling behaviour of SPI–MTGase hydrogels over time (1, 3, 6, 24, 48, and 72 hours). The 10% w/v SPI hydrogels exhibited a lower swelling degree compared to the 12% w/v SPI hydrogels at all time points. Moreover, for both SPI concentrations, hydrogels crosslinked with lower MTGase levels showed a higher swelling percentage at each evaluated time point. **c)** The release of SPI due to hydrolytic degradation was quantified using a BCA assay over time (1, 3, 6, 24, 48, and 72 hours). The left panel shows the release of SPI from 10% w/v SPI, 20 or 40 mg of MTGase/g SPI. The right panel shows the release of SPI from 12% w/v SPI, 20 or 40 mg of MTGase/g SPI. Both 10% and 12% w/v SPI hydrogels showed ~35% degradation within 24 hours, after which the concentration stabilized at around 2000 µg/mL in water. Data are presented as the mean ± SD of at least three replicates.

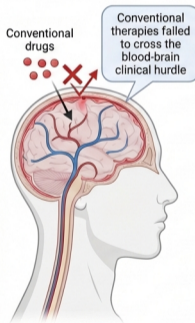
Figure SI 3



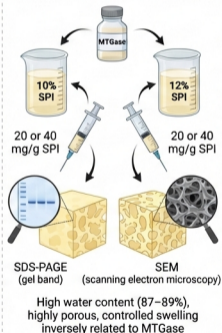
**Figure SI 3 Characterization of liposomes and their release from hydrogels. a)** Physicochemical parameters of liposomes measured by DLS and Z-Pals devices. Data are expressed as a mean ± standard deviation. HDs, hydrodynamic diameter; PDI, polydispersity index. **b)** Release kinetics of liposomes from 10% w/v SPI, 20mg of MTGase/g SPI hydrogels at different times, at 37 °C. These results were obtained by measuring the number of liposomes released by NanoSight technology NTA. Data are expressed as a mean ± standard deviation.

## MTGase-Crosslinked Soy Protein Isolate Hydrogels for Local Drug Delivery in Brain Tumor Therapy

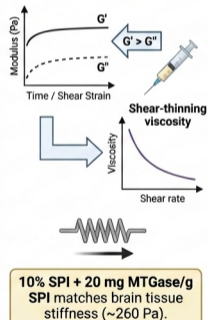
### Clinical Hurdle



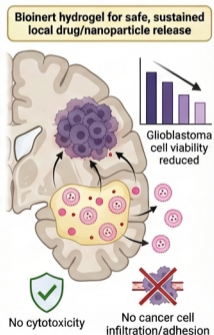
### Hydrogel Formulation & Characterization



### Mechanical & Injectable Properties



### Therapeutic Function & Biocompatibility



**MTGase-crosslinked SPI hydrogels are injectable, biocompatible, and enable sustained delivery of nanoparticles/drugs to brain tumors, bypassing the BBB and reducing tumor cell viability in vitro.**